BJP British Journal of Pharmacology

DOI:10.1111/bph.13166
www.brjpharmacol.org

RESEARCH PAPER

Simvastatin alleviates cardiac fibrosis induced by infarction via up-regulation of TGF-β receptor III expression

Correspondence
Yanjie Lu and Wenfeng Chu, Xuefu Road 194, Harbin, Heilongjiang 150081, China.
E-mail: yjlu86@163.com; cwf76928@aliyun.com

*These authors contributed equally to this study.

Received
2 October 2014
Revised
6 April 2015
Accepted
7 April 2015

Fei Sun[1]*, Wenqi Duan[1]*, Yu Zhang[1]*, Lingling Zhang[1], Muge Qile[1], Zengyan Liu[1], Fang Qiu[1], Dan Zhao[2], Yanjie Lu[1] and Wenfeng Chu[1]

[1]*Department of Pharmacology (The State-Province Key Laboratories of Biomedicine-Pharmaceutics of China, Key Laboratory of Cardiovascular Research, Ministry of Education), Harbin Medical University, Harbin, Heilongjiang, China,* [2]*Departments of Clinical Pharmacy and Cardiology, The 2nd Affiliated Hospital, Harbin Medical University, Key Laboratories of Education Ministry for Myocardial Ischemia Mechanism and Treatment, Harbin, Heilongjiang, China*

BACKGROUND AND PURPOSE

Statins decrease heart disease risk, but their mechanisms are not completely understood. We examined the role of the TGF-β receptor III (TGFBR3) in the inhibition of cardiac fibrosis by simvastatin.

EXPERIMENTAL APPROACH

Myocardial infarction (MI) was induced by ligation of the left anterior descending coronary artery in mice given simvastatin orally for 7 days. Cardiac fibrosis was measured by Masson staining and electron microscopy. Heart function was evaluated by echocardiography. Signalling through TGFBR3, ERK1/2, JNK and p38 pathways was measured using Western blotting. Collagen content and cell viability were measured in cultures of neonatal mouse cardiac fibroblasts (NMCFs). Interactions between TGFBR3 and the scaffolding protein, GAIP-interacting protein C-terminus (GIPC) were detected using co-immunoprecipitation (co-IP). *In vivo*, hearts were injected with lentivirus carrying shRNA for TGFBR3.

KEY RESULTS

Simvastatin prevented fibrosis following MI, improved heart ultrastructure and function, up-regulated TGFBR3 and decreased ERK1/2 and JNK phosphorylation. Simvastatin up-regulated TGFBR3 in NMCFs, whereas silencing TGFBR3 reversed inhibitory effects of simvastatin on cell proliferation and collagen production. Simvastatin inhibited ERK1/2 and JNK signalling while silencing TGFBR3 opposed this effect. Co-IP demonstrated TGFBR3 binding to GIPC. Overexpressing TGFBR3 inhibited ERK1/2 and JNK signalling which was abolished by knock-down of GIPC. *In vivo*, suppression of cardiac TGFBR3 abolished anti-fibrotic effects, improvement of cardiac function and changes in related proteins after simvastatin.

CONCLUSIONS AND IMPLICATIONS

TGFBR3 mediated the decreased cardiac fibrosis, collagen deposition and fibroblast activity, induced by simvastatin, following MI. These effects involved GIPC inhibition of the ERK1/2/JNK pathway.

Abbreviations

co-IP, co-immunoprecipitation; EF, ejection fraction; FS, fractional shortening; GIPC, GAIP-interacting protein C-terminus; IVSd, interventricular septal dimension in diastole; IVSs, interventricular septal dimension in systole; LAD, left anterior descending artery; Lenti-shNC, lentivirus with negative control short hairpin RNA; Lenti-shTR3, lentivirus with TGFBR3 short hairpin RNA; LVIDd, left ventricular internal dimension diastole; LVIDs, left ventricular internal dimension systole; MI, myocardial infarction; NMCF, neonatal mouse cardiac fibroblast; TGFBR3, TGF-β receptor III

Tables of Links

TARGETS
Catalytic receptors[a]
TGFR3, TGF-β receptor III
Enzymes[b]
ERK1/2
JNK
p38

LIGANDS
Simvastatin
TGF-β

These Tables list key protein targets and ligands in this article which are hyperlinked to corresponding entries in http://www.guidetopharmacology.org, the common portal for data from the IUPHAR/BPS Guide to PHARMACOLOGY (Pawson *et al.*, 2014) and are permanently archived in the Concise Guide to PHARMACOLOGY 2013/14 ([a,b]Alexander *et al.*, 2013a,b).

Introduction

Cardiac fibrosis is one of the most common manifestations of post-infarct cardiac remodelling. It is characterized by fibroblast over-proliferation and interstitial collagen deposition. In response to myocardium infarction, the dead myocardium is replaced with fibrotic scar tissues formed by fibroblasts and progressively loses contractile function, which ultimately leads to heart failure (Kong *et al.*, 2014).

Statins, inhibitors of hydroxymethylglutaryl CoA reductase, restrict cholesterol biosynthesis and have been widely used to treat hypercholesterolemia by lowering total and LDL cholesterol levels (Olyaei *et al.*, 2011). Apart from lipid-lowering, other effects on inflammation and cancer confirm the pleiotropic regulation of cell homeostasis by statins (Desai *et al.*, 2013). For instance, statins have been demonstrated to induce apoptosis of lymphoma cells by stimulating the p38 pathway (Qi *et al.*, 2013). Also, statins inhibited proliferation of cancer cells and human airway smooth muscle cells (Takeda *et al.*, 2006; Sanchez *et al.*, 2008). Moreover, the heart-protective effect of statins has been reported. Rosuvastatin improved heart function in patients suffering from congestive heart failure (CHF) due to ischaemia heart disease (Cleland *et al.*, 2009). Simvastatin attenuated the CHF-induced atrial structural remodelling and atrial fibrillation promotion in dogs, and its mechanism may be due to statin-induced inhibition of profibrotic atrial fibroblast responses and attenuation of left ventricular dysfunction (Shiroshita-Takeshita *et al.*, 2007). However, intensive investigations need to be carried out to elucidate the role of statins in mediating the development of cardiac fibrosis.

The TGF-β receptor III (TGFBR3) is an 851-amino-acid transmembrane proteoglycan that is involved in cellular homeostasis, differentiation, proliferation and apoptosis. In some cases, TGFBR3 binds to TGF-β and activates the downstream Smad signalling pathway (Esparza-Lopez *et al.*, 2001). Recently, we have demonstrated that TGFBR3 functioned as an inhibitor of the TGF-β1/TGF-β2 receptor complex and TGF-β1 expression (Chu *et al.*, 2011), and we further identified TGFBR3 as a key anti-fibrosis factor via its inhibition of TGF-β1 signalling (Liang *et al.*, 2012). Here we studied whether TGFBR3 participated in the regulation of cardiac fibrosis by statins. Our data have disclosed a novel mechanism by which simvastatin restricted post-infarct cardiac fibrosis by up-regulating TGFBR3, thereby suppressing ERK1/2 and JNK-dependent fibroblast activity and collagen production.

Methods

Mouse models of myocardial infarction (MI)

All animal care and experimental protocols were in accordance with the Institutional Animal Care, which was approved by the Ethics Committee of Harbin Medical University, China. All studies involving animals are reported in accordance with the ARRIVE guidelines for reporting experiments involving animals (Kilkenny *et al.*, 2010; McGrath *et al.*, 2010). A total of 70 animals were used in the experiments described here.

Male Kunming mice weighing 20–25 g were housed in the environment at a temperature of 20°C with a 12/12 h light/dark cycle. Mice were pretreated with simvastatin (0.5 $mg \cdot g^{-1} \cdot day^{-1}$; Sigma-Aldrich Co., LLC, St. Louis, MO, USA) via an intragastric tube for 7 days. Mice were anaesthetized with pentobarbital sodium (40 $mg \cdot kg^{-1}$, i.p.), the skin of the chest was shaved and disinfected. The mice were intubated and ventilated with an artificial respiration machine (UGO Basile S.R.L. Biological Research Apparatus, Ugo Basile, Milan, Italy). An incision was performed through the fourth intercos-

tal space and the heart was exposed. The left anterior descending coronary (LAD) artery was ligated with 7/0 silk thread. One, 7 or 28 days later, the mice were killed (sodium pentobarbitone, 40 mg kg^{-1} and xylazine, 12.5 mg kg^{-1}, i.p.). and the heart dissected for ischaemia zone, border zone and non-ischaemia zone. For control mice, a suture was passed through the myocardium around the LAD artery without ligation.

In vivo *lentivirus carrying shRNA for TβRIII infection*

The lentivirus-mediated shRNA for TGFBR3 (Lenti-shTR3) (5′ CACC GGGA GGTT CACA TCCT AAAC GAAT TTAG GATG TGAA CCTCCC3′) and the lentivirus carrying scrambled shRNA (Lenti-shNC) (5′GTTC TCCG AACG TGTC ACGT3′) as negative control were synthesized by Invitrogen (Shanghai, China). Briefly, mice were anaesthetized, a thoracotomy was performed through the fourth intercostal space. The ascending aortic artery and the main pulmonary artery were clamped. The lentivirus was injected (2.5 × 10E7 TU·mL^{-1} at volume of 100 μL) through the tip of the heart into the left ventricular cavity. The arteries were occluded for 10 s after lentivirus injection. Treatment with simvastatin was started 7 days after lentivirus injection. After treatment, GFP fluorescence in cryosections of the hearts injected with lentivirus was measured by laser scanning confocal microscopy (FV300; Olympus Medical System, Tokyo, Japan).

Isolation of cardiac fibroblasts

The hearts of neonatal Kunming mice (1–3 days old) were excised and cut into small pieces as described previously (Li *et al.*, 2013). Cardiac fibroblasts were isolated using a 0.25% solution of trypsin and were cultured in 6-well plates containing DMEM (HyClone, Logan, UT, USA) with 10% FBS (HyClone) at 37°C in 5% CO_2, 95% air for 48 h before experiments.

Drug administration and transfection of cardiac fibroblasts

Simvastatin was dissolved in DMSO and cells were treated with simvastatin at 1, 5 or 10 μM (final concentration of DMSO was 1%). To induce cell fibrosis, 20% FBS was added to DMEM when cardiac fibroblasts were cultured (Chu *et al.*, 2011).

Targeting siRNAs and the negative control siRNA were purchased from GenePharma (Shanghai, China). The target sequence of TGFBR3 was sense, 5′ GGGA GGUU CACA UCCU AAATT3′, and antisense, 5′ UUUA GGAU GUGA ACCU CCCTT3′. The target sequence of GAIP-interacting protein C-terminus (GIPC) was sense: 5′ GCAG UGUG AUUG ACCA CAUTT3′, and antisense: 5′AUGU GGUC AAUC ACAC UGCTT3′. Pc-DNA3.1-mTGFBR3 plasmid (GeneChem Co., Ltd, Shanghai, China) and pc-DNA3.1-plasmid (GeneChem Co., Ltd) as an empty vector were all transfected with X-tremeGENE siRNA transfection reagent (Roche Molecular Biochemicals, Mannheim, Germany) for 48 h.

Transmission electron microscopy

Briefly, the samples were fixed in phosphate-buffered 2.5% glutaraldehyde (pH 7.4) at 4°C overnight and immersion postfixed in 0.1 M cacodylate buffer with 1% osmium tetroxide for 1 h (Li *et al.*, 2013). Then samples were dehydrated through a graded ethanol series, embedded in Epon medium and dissected into 60–70 nm sections. Sections were stained with uranyl acetate and lead citrate and were observed with a JEOL 1200 electron microscope (JEOL Ltd, Tokyo, Japan).

Masson staining

Hearts were sectioned and immersed in 10% neutral buffered formalin for 24 h, then stained with Masson's Trichrome (Accustain HT15; Sigma-Aldrich, St. Louis, MO, USA). The extent of collagen deposition was calculated with image analysis software (Image-Pro Plus v4.0; Meida Cybernetics, Bethesda, MD, USA) as previously described (Li *et al.*, 2013).

Measurement of cell viability

Cells were seeded into a 96-well microplate at 10 000 cells per well in 100 μL of medium and treated as described. Cells were incubated with 10 μL MTT [3-(4,5-dimethylthiazol-2-yl)-2,5-diphenyl-2H-tetrazolium bromide] solution (Sigma-Aldrich) (0.5 mg·mL^{-1}) for 4 h. Each well received 100 μL of DMSO to dissolve the formazan, and the plate was shaken for 10 min. The absorbance for each well was measured at 490 nm using a microplate spectrophotometer (Tecan Austria GmbH, Untersbergstrasse, Austria).

Measurement of collagen content

A Sircol Collagen Assay kit (Biocolor Ltd., Northern Ireland, UK) was used to determine the total collagen content. Briefly, 0.05 M Tris buffer (pH 7.5) was used to lyse cells, and 1 mL of Sircol Dye reagent was used to stain the lysate (100 mL). Contents were mixed for 30 min and centrifuged for 10 min (at >10 000× *g*) to pellet the bound dye. Each tube received 1 mL of the alkali reagent to dissolve the bound dye, and the absorbance value was read at 540 nm. Collagen content (mg) was converted to protein units using the linear calibration curve generated from standards (Vitrogen 100; Angiotech Biomaterials, Palo Alto, CA, USA) and was normalized to the total protein (mg) of each sample.

Western blotting

Total protein was extracted from cells or tissues and its concentration was determined using a bicinchoninic acid kit. The samples were boiled for 5 min and loaded at 80 μg per lane. The Western blotting procedures were as previously described (He *et al.*, 2014). GAPDH was used as the internal control. The antibody sources were as follows: anti-TGFBR3, anti-phospho-p38, anti-phospho-ERK1/2, anti-phospho-JNK, anti-p38, anti-ERK1/2, anti-JNK (1:1000 dilution; Cell Signalling Technology, Beverly, MA, USA), anti-GIPC1 (1:150 dilution; Santa Cruz Biotechnology, Inc., Santa Cruz, CA, USA) and anti-GAPDH (1:500 dilution; Research Diagnostics, Concord, MA, USA).

Co-immunoprecipitation

For co-immunoprecipitation (co-IP), cells or tissues were lysed in RIPA buffer (Beyotime, Shanghai, China) and then centrifuged at 12 000× *g* for 15 min. The supernatant was collected and aliquoted into three parts for control input, primary antibody and control IgG. The primary antibody and IgG were incubated with protein A/G agarose beads at 4°C overnight on a shaker. After the incubation, the samples were centrifuged at 3000× *g* for 5 min, and the beads were collected

and washed with PBS three times. The appropriate amount of loading buffer was added to the beads, which were boiled for 5 min and then centrifuged at 12 000× *g* for 5 min to dissociate the proteins from the beads. The IP products were subsequently analysed using Western blotting.

Echocardiographic measurement

To test left ventricular function, transthoracic echocardiography was performed using an ultrasound machine (Vivid 7 GE Medical; GE Healthcare, Horten, Norway) with a 10 MHz phase-array transducer as previously described (Pan *et al.*, 2012).

Data analysis

The data are presented as the means ± SEM and were processed with GraphPad Prism 5.0. One-way ANOVA with Bonferroni's *post hoc* test was used for multiple comparisons. A two-tailed value of $P < 0.05$ was considered statistically significant.

Results

Simvastatin attenuates myocardial fibrosis and improves cardiac function in mice after MI induction

First, to detect the effect of simvastatin on cardiac fibrosis, mice were pretreated with simvastatin or normal saline for 7 days and were subjected to LAD ligation for 1 week or 4 weeks. The tissues of the border zone of the infarct were then subjected to collagen staining and electron microscopy to determine the effects of simvastatin on collagen production and fibroblast activity respectively.

Masson staining showed that 7 day infarction induced massive collagen production and that simvastatin pretreatment alleviated the MI-induced collagen deposition by 67% (Figure 1). Similar results were observed in electron micrographs. In the control groups, the myocardium presented an orderly myofibril distribution, collagen in myocardial interval was rarely seen, and fibroblasts were in a quiescent state. In the MI groups, cardiomyocytes presented fractured mitochondrial cristae, disorderly sarcomere structures and an interstitial space filled with massive fasciculate collagen and active fibroblasts. In the simvastatin-treated groups, less collagen was deposited, and fibroblasts were quiescent (Figure 1). The lower degree of infarction injury in simvastatin-treated mice indicated that simvastatin partly protected the heart from the MI insult, which was manifested as a decrease in interstitial collagen deposition and fibroblast activity. Table 1 presents the echocardiographic parameters evaluated in the three groups of mice after 4 week MI. The increased interventricular septal thickness in diastole (IVSd), the interventricular septal thickness in systole (IVSs), the left ventricular internal dimension diastole (LVIDd) and the left ventricular internal diameter in systole (LVIDs) with decreased fractional shortening (FS) and ejection fraction (EF) values confirmed the myocardial fibrosis. Simvastatin-treated mice exhibited reversal of FS and EF. The changes in heart function indicate that simvastatin may regulate cardiac fibrosis and the unchanged parameters are consistent with the reports that simvastatin has no effect on hypertrophy (Hermida *et al.*, 2013).

Simvastatin up-regulates TGFBR3 and suppresses ERK1/2 and JNK pathways in vivo

TGFBR3, a glycosaminoglycan transmembrane receptor, inhibits collagen production by reducing TGF-β1 signalling activity and is closely involved in the development of cardiac fibrosis (Liang *et al.*, 2012). We further noted that TGFBR3 was involved in MI injury because of the decreased level of TGFBR3 after 24 h of MI. However, TGFBR3 was up-regulated nearly 1.33-fold in MI mice with simvastatin pretreatment (Figure 2A).

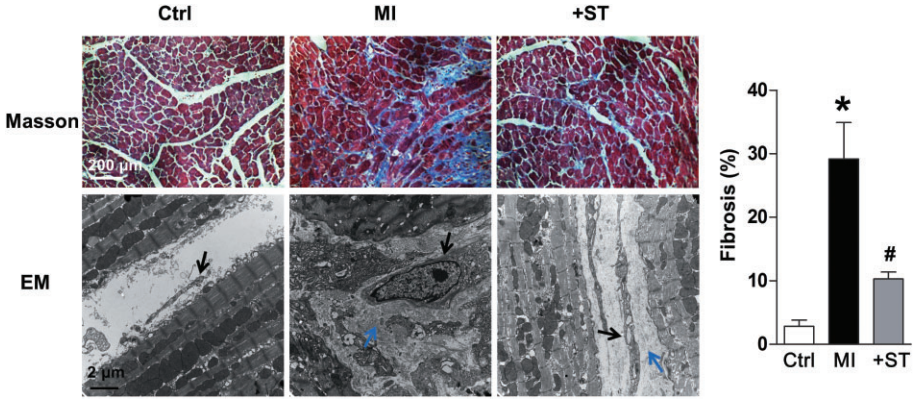

Figure 1

Simvastatin reduces cardiac fibrosis in ventricular tissue of mice following MI. Mice were pretreated with simvastatin (ST; 0.5 mg·g^{-1}·day^{-1}) for 7 days and the LAD ligated for 1 week. Collagen deposition and ultrastructure were determined by Masson staining and electron microscopy (EM). Microscope images show a thicker collagen fibre pattern (blue) in the MI groups than in the control groups, and simvastatin reduced this intense collagen deposition. Representative images from electron microscopy: (i) control: black arrow indicates normal cardiac fibroblasts; (ii) MI: excessive proliferation of cardiac fibroblasts and collagen deposition (blue); (iii) simvastatin-treated: quiescent cardiac fibroblasts and less collagen deposition. Ctrl, control; ST, simvastatin; EM, electron microscopy. *$P < 0.05$ versus control group; #$P < 0.05$ versus MI group. $n = 6$.

Table 1

Echocardiographic parameters in 4-week-old control (Ctrl), MI and MI+ simvastatin (+ST) groups of mice

Group	Ctrl (n = 6)	MI (n = 6)	+ST (n = 6)
IVSd (mm)	0.82 ± 0.20	1.12 ± 0.13*	1.11 ± 0.38
IVSs (mm)	1.24 ± 0.22	1.57 ± 0.21*	1.72 ± 0.54
LVIDd (mm)	3.64 ± 0.38	4.74 ± 0.80*	4.62 ± 0.56
LVIDS (mm)	2.31 ± 0.34	3.86 ± 0.81*	3.34 ± 0.43
LVPWd (mm)	0.82 ± 0.18	0.68 ± 0.18	1.12 ± 0.32
LVPWs (mm)	1.16 ± 0.24	0.83 ± 0.28	1.41 ± 0.45
FS (%)	36.8 ± 3.6	19.2 ± 4.1*	27.5 ± 10.3#
EF (%)	67.5 ± 4.9	39.3 ± 7.8*	52.9 ± 10.3#

*P < 0.05 versus control group; #P < 0.05 versus MI group. n = 6.
LVPWd, left ventricular posterior wall thickness at end-diastole; LVPWs, left ventricular posterior wall thickness at end-systole.

Notably, the ERK1/2 pathway is involved in the expression of collagen genes in human peritoneal mesothelial cells and is involved in collagen type I transcriptional activation of fibroblasts derived from aged murine hearts. The specific ERK1/2 inhibitor PD98059 suppresses collagen I mRNA expression after TGF-β1 treatment in human peritoneal mesothelial cells (Hung *et al.*, 2001a). Additionally, JNK phosphorylation is associated with augmented proliferation and collagen production in renal fibroblasts (Sun *et al.*, 2013). In our experiments, the activities of the ERK1/2 and JNK pathways correlated closely with the severity of cardiac fibrosis, and MI up-regulated ERK1/2 and JNK phosphorylation, whereas simvastatin depressed this increased phosphorylation (Figure 2B and D). MI also activated the p38 pathway, but this pathway was not altered significantly after simvastatin (Figure 2C).

The inhibitory effects of simvastatin on cell proliferation and collagen content are mediated by elevated TGFBR3 expression in neonatal mouse cardiac fibroblasts (NMCFs)

TGFBR3 appears to function as an inhibitor of cardiac fibrosis via several mechanisms (Ezquerro *et al.*, 2003; Hermida *et al.*, 2009). To test whether raised levels of TGFBR3 were critical to simvastatin-induced anti-fibrosis in infarcted heart, we treated NMCFs with various doses of simvastatin for 24 h. TGFBR3 was then detected using Western blotting (Figure 3A), which revealed that TGFBR3 expression increased in a dose-dependent manner. The TGFBR3 level was increased to twice that of the control group by 5 μM simvastatin and to 2.5-fold by 10 μM simvastatin. The effect of simvastatin on TGFBR3 expression indicated that TGFBR3 was involved in the signalling pathway that underlies simvastatin's anti-fibrotic action.

Given these results, we used siRNA to block TGFBR3 expression in NMCFs. The degree of TGFBR3 knock-down is shown in Figure 3B. As Figure 3C shows, the increase in total collagen content induced by FBS stimulation was prevented by 10 μM simvastatin. Strikingly, TGFBR3 knock-down reversed this inhibition of collagen by simvastatin.

Fibroblast over-proliferation is a characteristic finding in cardiac fibrosis and contributes greatly to its pathogenesis. Therefore, fibroblast proliferation reflects cardiac fibrosis injury. We measured NMCF proliferation via MTT assay and found that, as shown in Figure 3D, FBS promoted over-proliferation whereas simvastatin eliminated this effect. As expected, this suppression of cell proliferation was abolished by TGFBR3 knock-down. These results confirmed that simvastatin inhibited NMCF proliferation and that TGFBR3 was an important factor in the regulation of fibroblast proliferation by simvastatin.

Knock-down of TGFBR3 abolishes the inhibitory role of simvastatin in regulating ERK1/2 and JNK activation in NMCFs

To detect whether ERK1/2 or JNK signalling acts downstream of TGFBR3, cells transfected with TGFBR3 siRNA or negative control siRNA were treated with simvastatin or FBS. Enhanced ERK1/2 phosphorylation was observed in the FBS group, which was further increased by TGFBR3 siRNA (Figure 4A). Furthermore, simvastatin partly inhibited ERK1/2 phosphorylation whereas TGFBR3 knock-down cancelled the inhibitory effect of simvastatin on ERK1/2 signalling (Figure 4C). Similar results were observed in JNK signalling (Figure 4B and D). Thus, the decreased activation of the ERK1/2 and JNK pathways induced by simvastatin was dependent on the presence of TGFBR3.

TGFBR3 inhibits ERK1/2 and JNK signalling by interacting with GIPC

The PDZ-protein GIPC interacts with TGFBR3 to stabilize TGFBR3 at the cell surface and enhance TGF-β signalling (Blobe *et al.*, 2001; Sanchez *et al.*, 2011). Moreover, regulation of breast cancer progression and epithelial-mesenchymal transformation requires TGFBR3 interaction with GIPC (Lee *et al.*, 2010; Sanchez *et al.*, 2011; Townsend *et al.*, 2012). However, the mechanism by which TGFBR3-GIPC mediates cell activity is poorly understood. Interestingly, investigations regarding the association between GIPC and the ERK1/2

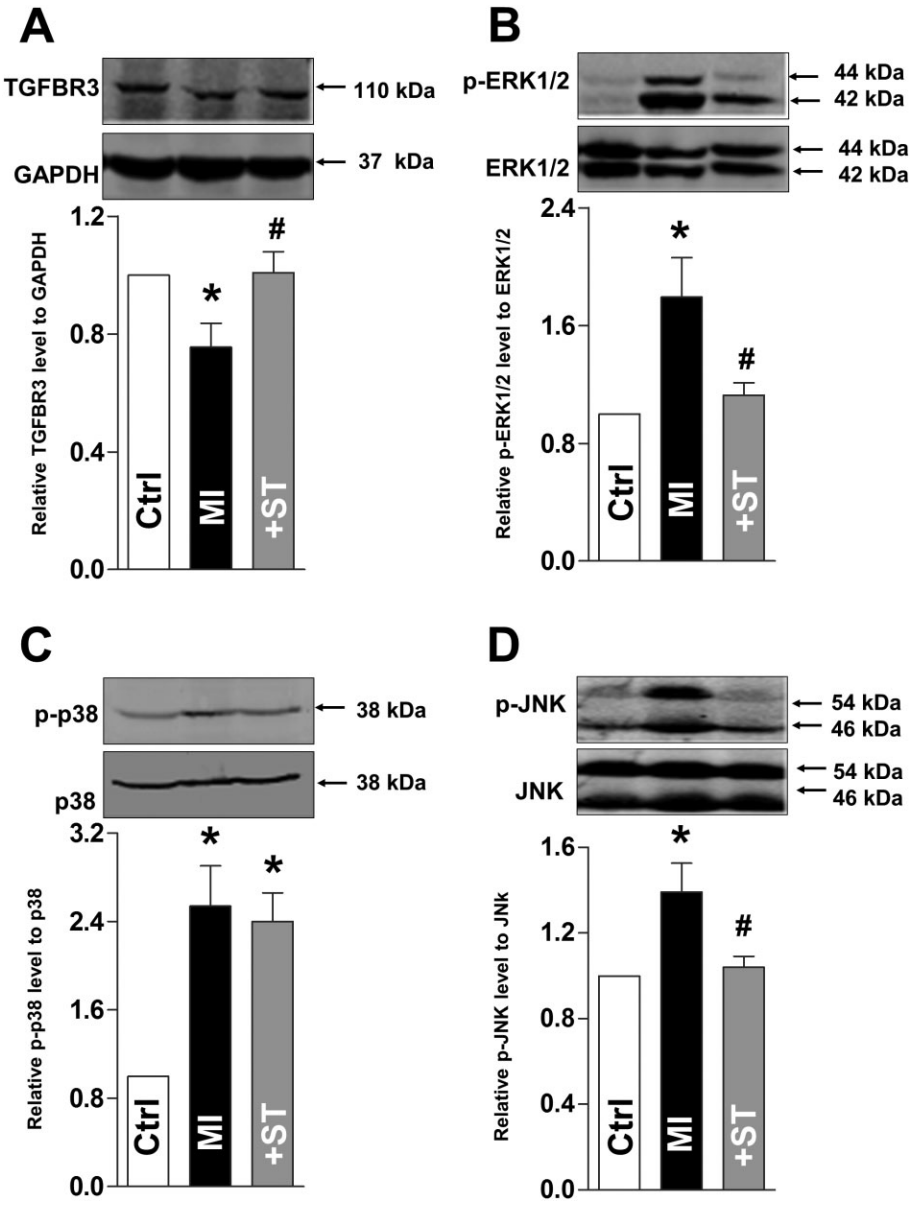

Figure 2

Simvastatin alters TGFBR3 expression and MAPK phosphorylation *in vivo*. Mice were pretreated with simvastatin (ST; 0.5 $mg \cdot g^{-1} \cdot day^{-1}$) for 7 days and the LAD ligated for 1 day. TGFBR3(A), ERK1/2 and p-ERK1/2 (B), p38 and p-p38 (C) and JNK and p-JNK (D) were measured using Western blotting. Data are presented relative to control (Ctrl) and are shown as the means ± SEM. *$P < 0.05$ versus control group; #$P < 0.05$ versus MI group. $n = 6$.

pathway have indicated a role for GIPC in a TGFBR3-ERK1/2 pathway (Hu *et al.*, 2003). To confirm the interaction between TGFBR3 and GIPC, we performed co-IP (Figure 5A). NMCFs were co-transfected with pc-DNA3.1-mTGFBR3 plasmid and GIPC siRNA for 48 h. The transfection efficiencies are shown in Figure 5B and C. Western blotting revealed that TGFBR3 overexpression decreased ERK1/2 and JNK pathway activities by 60%, whereas treatment with the siRNA for GIPC restored the activities to control levels (Figure 5D and E). These results suggest that the interaction between TGFBR3 and GIPC was essential for the activation of the ERK1/2 and JNK pathways.

Lentivirus-mediated TGFBR3 silencing reverses anti-fibrotic effect by simvastatin in vivo

To determine the role of TGFBR3 in the modulation of cardiac fibrosis by simvastatin *in vivo*, Lenti-shTR3 was injected into the myocardium to knock-down TGFBR3 in cardiac fibroblasts. Mice were then treated with simvastatin and the LAD was ligated. The border tissues of the resulting infarct were examined. Knock-down of TGFBR3 in cardiac fibroblasts was confirmed by Western blotting and

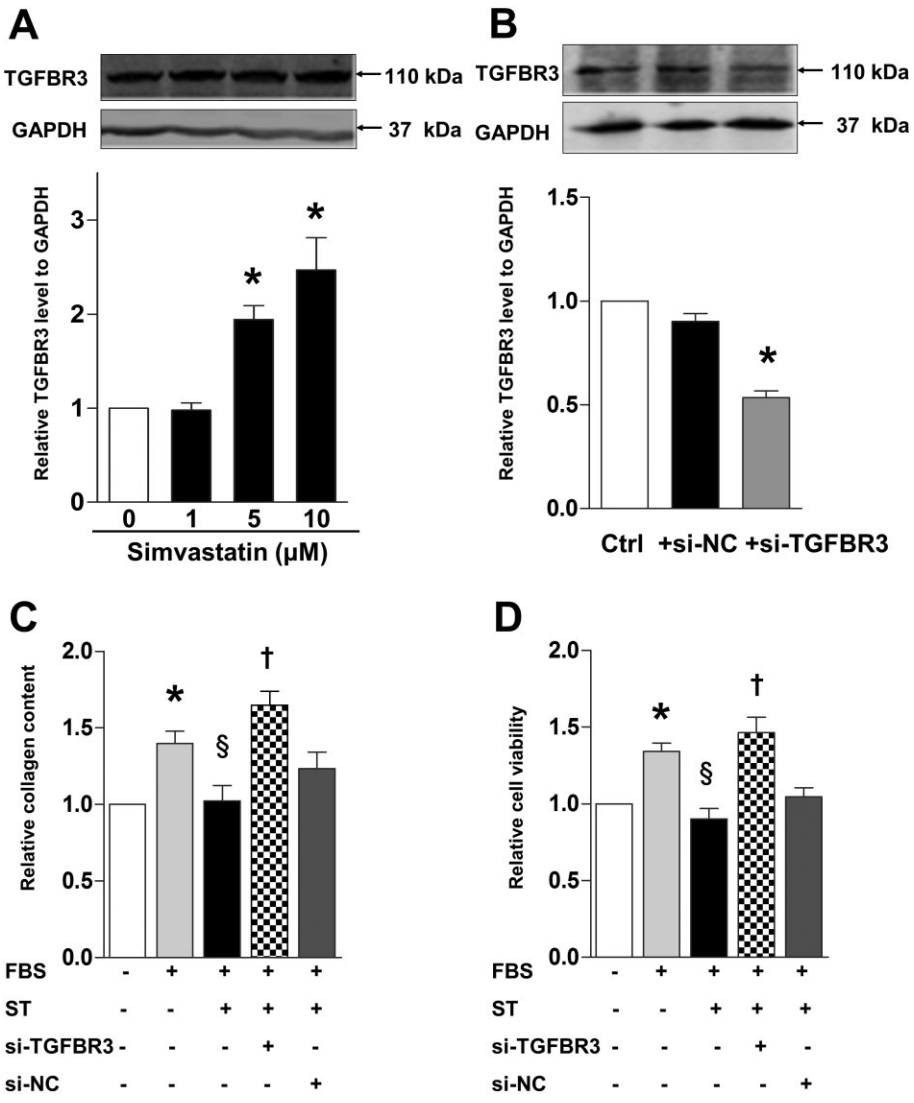

Figure 3

Identification of TGFBR3 as a novel target of the inhibitory effects of simvastatin on collagen content and cell proliferation. (A) Cultured NMCFs were incubated for 2 h with 1, 5 or 10 μM simvastatin (ST). (B, C, D) NMCFs were transfected with TGFBR3 siRNA for 48 h and then incubated for 2 h with 10 μM simvastatin or 20% FBS for 2 h. Collagen production was assayed with a Sircol Collagen Assay kit (C) and proliferation of NMCFs by MTT assay (D). Western blotting was used to determine TGFBR3 expression. Data are shown as the means ± SEM. *$P < 0.05$ versus control group; §$P < 0.05$ versus FBS treatment alone; †$P < 0.05$ versus FBS+ST+si-NC. $n = 5$.

fluorescence (Supporting Information Fig. S1). Knock-down of TGFBR3 also reduced the anti-fibrotic effect of simvastatin in the infarcted heart. Masson staining exhibited up-regulated collagen staining in Lenti-shTR3 group compared with Lenti-shNC group after 7 day MI. Electron micrographs showed more serious injury of MI in the shTGFBR3 group, with marked deposits of fasciculate collagen and hypertrophied and activated fibroblasts (Figure 6A). Heart function evaluated by echocardiography showed that FS and EF were lower in Lenti-shTR3 group after 7 days of MI (Figure 6B), indicating the critical contribution of TGFBR3 to the improvement in heart function after simvastatin. These results suggest that TGFBR3 is a critical component of the procesess whereby simvastatin protects against cardiac fibrosis, decreases collagen deposition and inhibits fibroblast activity.

Consistent with the results *in vitro*, the interaction between TGFBR3 and GIPC *in vivo* was confirmed by co-IP (Figure 6C). Furthermore, border tissue exhibited more activated ERK1/2 and JNK pathway in Lenti-shTR3 group, but the p38 pathway was not altered significantly (Figure 6D–F). These results further indicate that the anti-fibrotic role of TGFBR3 in heart is mediated by GIPC to regulate ERK1/2 and JNK signalling pathways.

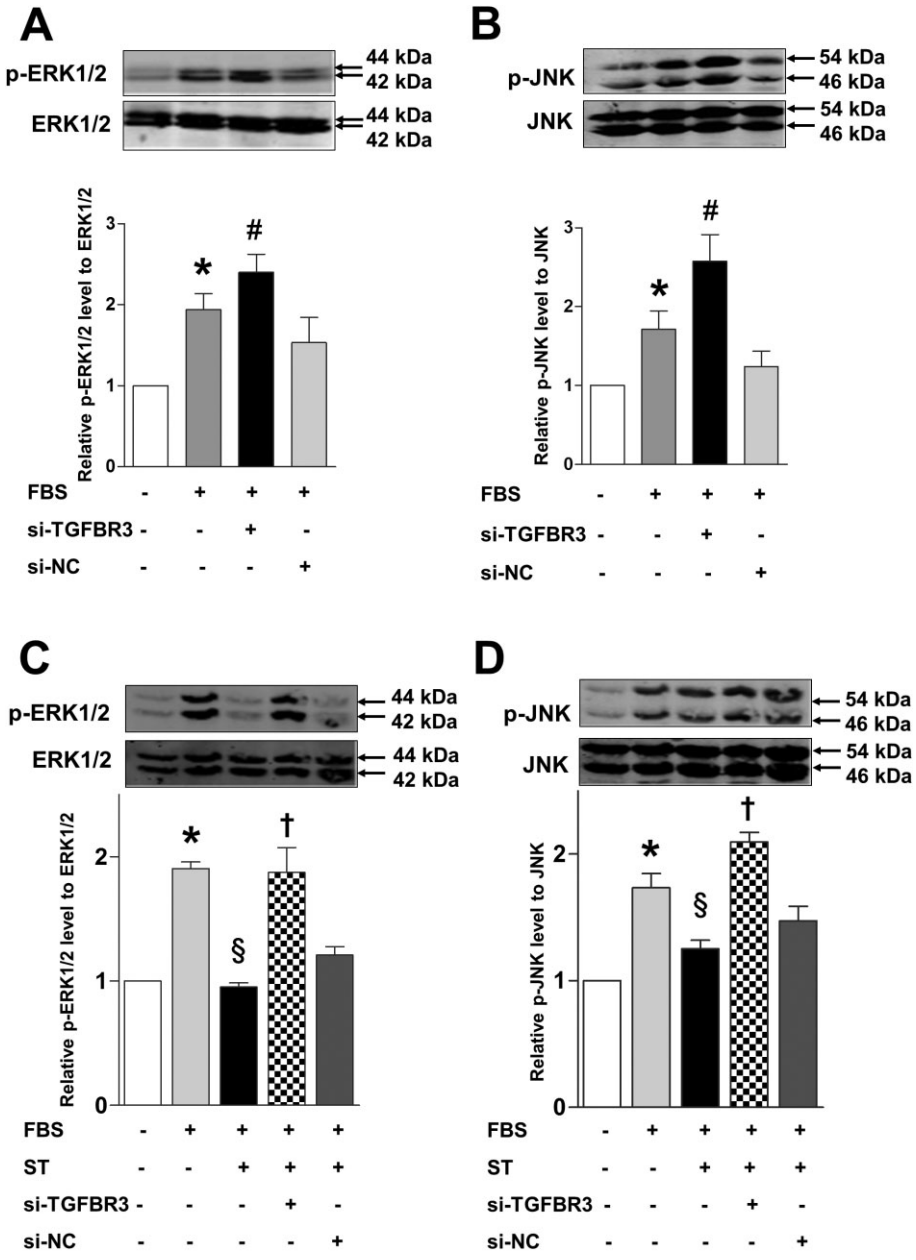

Figure 4

Silencing TGFBR3 restricts down-regulation of ERK1/2 and JNK phosphorylation by simvastatin. (A and B) NMFCs were transfected with TGFBR3 siRNA for 48 h and incubated for 2 h with 20% FBS. (C and D) NMCFs were transfected with TGFBR3 siRNA for 48 h, then incubated for 2 h with 10 μM simvastatin (ST) or with 20% FBS for 2 h. ERK1/2 and JNK phosphorylation was quantified using Western blotting. Data are shown as the means ± SEM. *$P < 0.05$ versus control group; §$P < 0.05$ versus FBS treatment alone; #$P < 0.05$ versus FBS+ si-NC; †$P < 0.05$ versus FBS+ST+si-NC. $n = 4$.

Discussion and conclusions

The current work provides strong evidence that TGFBR3 stimulated by simvastatin down-regulated the post-infarct accumulation of interstitial collagen and inhibited cardiac fibroblast activity, by interacting with GIPC to mediate MAPK (ERK1/2 and JNK) signalling (Figure 7). Thus, our current findings identified TGFBR3 as a worthwhile target in the anti-fibrotic effects of simvastatin in the heart.

Cardiac fibrosis that is caused by coronary artery stenosis-induced ischaemia and hypoxia triggers increases in heart volume and weight, along with fibroplasia and even transmural scarring, and ultimately causes arrhythmia and heart failure (Kong *et al.*, 2012). Pathological changes after MI due to occlusion of the LAD, show a long-term progression. In the rat MI model, for instance, fibroblast proliferation occurs at day 4 after MI and cardiac fibrosis is detected 7 days after MI. By day 28, the ischaemic heart develops significant

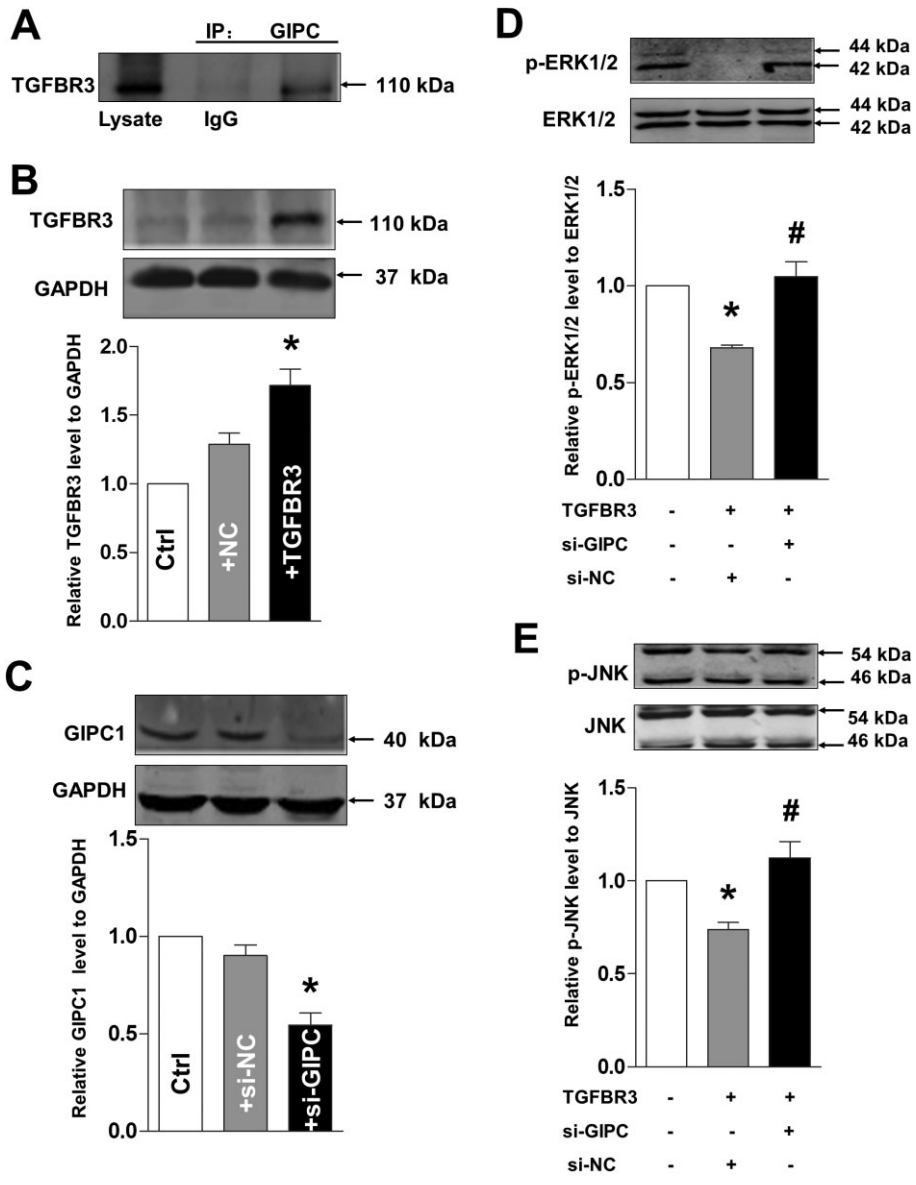

Figure 5

TGFBR3 interaction with GIPC is critical to the down-regulation of ERK1/2 and JNK signalling by simvastatin. (A) TGFBR3-GIPC complexes were measured by co-IP. (B–E) NMCFs were co-transfected with pc-DNA3.1-m TGFBR3 plasmid and GIPC1 siRNA for 48 h. TGFBR3 and GIPC expression and ERK1/2 and JNK phosphorylation were quantified using Western blot. Data are shown as the means ± SEM. *$P < 0.05$ versus control group; #$P < 0.05$ versus TGFBR3+si-NC. $n = 4$.

compensatory hypertrophy and, eventually, heart failure (Backlund *et al.*, 2004; Krzeminski *et al.*, 2008; Pan *et al.*, 2012).

Our investigation showed that simvastatin prevented the development of cardiac fibrosis by decreasing collagen production and fibroblast proliferation, consistent with previous reports. Rosuvastatin ameliorates chronic heart failure induced by ischaemic heart disease in humans (Cleland *et al.*, 2009; McMurray *et al.*, 2009; Askevold *et al.*, 2013). Compared with placebo, simvastatin decreased left ventricular mass, interventricular septal thickness and posterior wall thickness in a β-myosin heavy chain-Q transgenic rabbit model of human hypertrophic cardiomyopathy (Patel *et al.*, 2001). These findings agree with our observations from the treatment of mice with oral simvastatin. In the present study, after 7 or 28 days, our model of MI induced a significant loss of heart function, confirming the success of LAD ligation, and treatment with simvastatin decreased the cardiac fibrosis and improved cardiac dysfunction. The impaired FS and EF at day 28 demonstrate poor heart function and these parameters were particularly improved by simvastatin. Simvastatin, however, did not inhibit myocardial hypertrophy as seen from the unchanged IVSd, IVSs, LVIDd and LVIDs, which is consistent with earlier results showing no effect of statins on

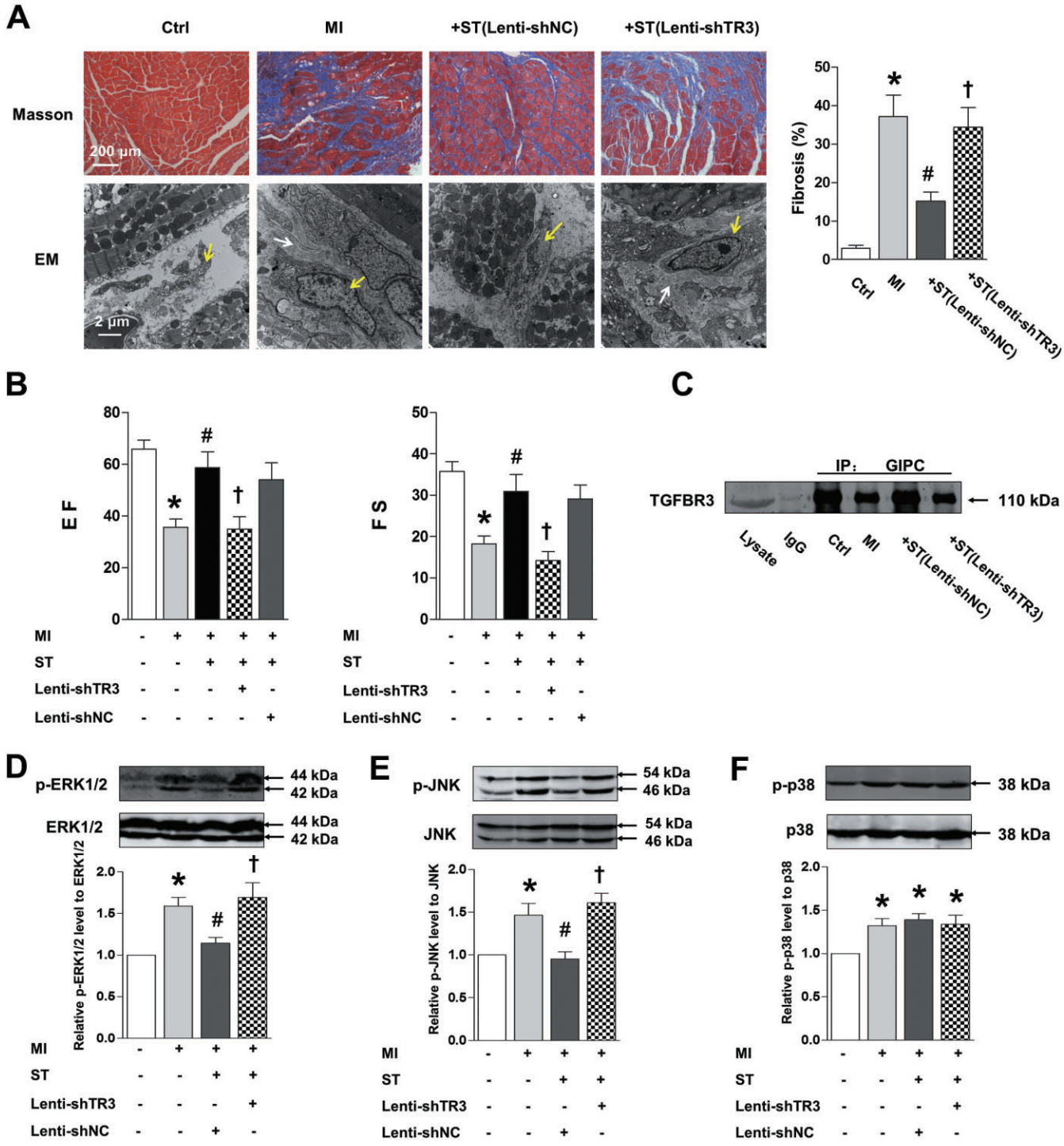

Figure 6

TGFBR3 interaction with GIPC is critical in simvastatin-attenuated cardiac fibrosis induced by LAD ligation. Mice that received lentivirus mediating shTGFBR3 or lentivirus mediating shNC were pretreated with simvastatin (ST; 0.5 mg·g^{-1}·day^{-1}) for 7 days and the LAD ligated for 1 week. (A) Collagen deposition and ultrastructure were evaluated by Masson staining and electron microscopy. Photomicrographs show thicker collagen fibre pattern (blue) in the MI groups than the one in the control groups, while simvastatin with Lenti-shNC reduced the intense collagen deposition and Lenti-shTR3 reversed the effect of simvastatin. Electron micrography showed representative results. (i) control: yellow arrow indicates cardiac fibroblasts; (II) MI: activated cardiac fibroblasts and extensive collagen deposition (white); (III) simvastatin with Lenti-shNC treated: less collagen deposition and fallow cardiac fibroblasts; (iv) simvastatin with Lenti-shTR3 treated: activated cardiac fibroblasts and thick collagen fibre pattern. (B) EF and FS were determined by echocardiography. (C) TGFBR3–GIPC interaction was measured by co-IP. (D–F) MAPK pathway was measured using Western blotting. Lenti-shTR3, lentivirus mediating sh-TGFBR3; Lenti-shNC, lentivirus mediating sh-NC. Data are shown as the means ± SEM. *P < 0.05 versus control group; #P < 0.05 versus MI group. †P < 0.05 versus MI+ST+Lenti-shNC. n = 7.

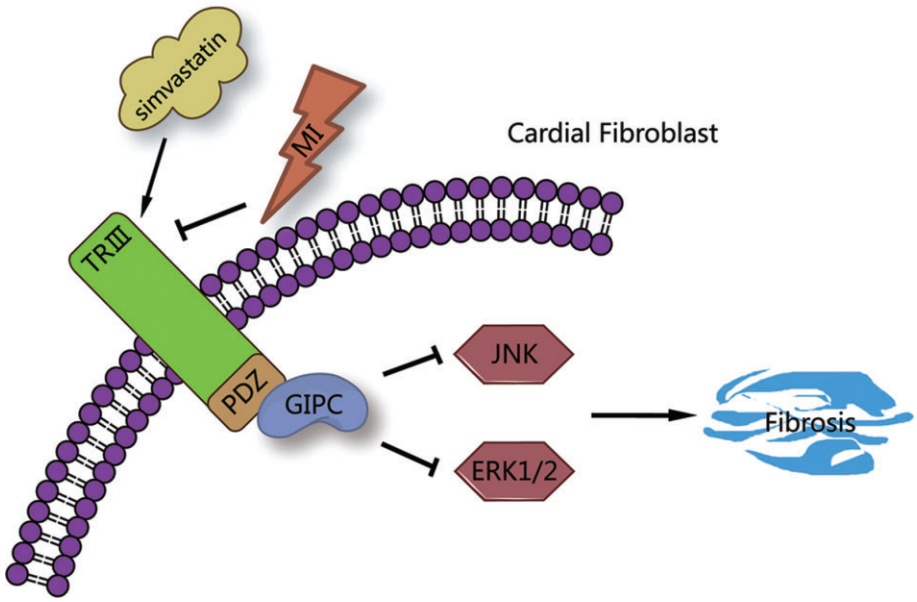

Figure 7

A diagram of the involvement of TGFBR3 in the inhibition by simvastatin of cardiac fibrosis induced by MI. Simvastatin repairs the dysfunctional TGFBR3 (TRIII) signalling induced by MI. TGFBR3 further interacts with GIPC, down-regulates ERK1/2 and JNK signalling pathways and consequently reduces cardiac fibrosis.

cardiomyocyte hypertrophy after 7 day MI (Hermida *et al.*, 2013). The present study combined with earlier studies confirmed that the protective effect of simvastatin is not through prevention of cardiomyocyte hypertrophy, but due to the amelioration of cardiac fibrosis (Shiroshita-Takeshita *et al.*, 2007; Hermida *et al.*, 2013).

Furthermore, in dogs subjected to ventricular tachypacing to induce CHF, simvastatin suppressed proliferation of atrial fibroblasts (Shiroshita-Takeshita *et al.*, 2007). Additionally, statins reduced pro-collagen type I production, α-smooth muscle actin expression and fibroblast migration by activating AMP-activated protein kinase in a mouse model of the metabolic syndrome (Hermida *et al.*, 2013). These findings are compatible with our observations that simvastatin suppresses MI-induced collagen production and fibroblast activity. Together, these results suggest that statins can be effective against myocardial remodelling. However, more investigations are needed to fully explain the mechanism(s) of the actions of statins.

We have focused on the mechanism of the anti-fibrotic effects of statins. After a 1 day MI injury, TGFBR3 expression declined, which was reversed by simvastatin, and simvastatin attenuated the activated ERK1/2 and JNK signalling. Atorvastatin down-regulates endoglin expression via PI-3 kinase, Akt and Smad3 phosphorylation (Shyu *et al.*, 2010). Endoglin is the related TGF-β superfamily co-receptor that shares a limited amino acid sequence identity with TGFBR3 and is expressed in some cell types which have little or no TGFBR3 expression, to compensate for its absence (Letamendia *et al.*, 1998; Gatza *et al.*, 2010). Interestingly, in cardiac fibroblasts, a synthetic peptide from TGFBR3, P144, reduced TGF-β1-dependent signalling and collagen I synthesis (Hermida *et al.*, 2009) and also reduced liver fibrogenesis in rats with CCl_4 liver injury (Ezquerro *et al.*, 2003). Furthermore, TGFBR3 overexpression inhibits miR-21 and collagen production in NMFCs (Liang *et al.*, 2012). All this evidence raised the possibility that TGFBR3 was the target of simvastatin in its anti-fibrotic actions. Our results showed that TGFBR3 knock-down prevented the down-regulation of collagen production and cell proliferation induced by simvastatin, confirming our hypothesis.

In addition to TGFBR3 expression, ERK1/2 and JNK signalling was activated after MI, whereas simvastatin reduced the levels of activated ERK1/2 and JNK. Interestingly, the MAPK pathway associated with the development of cardiac fibrosis has been reported in several studies (Ponticos *et al.*, 2009; Lagares *et al.*, 2010; Jang *et al.*, 2013). In human peritoneal mesothelial cells and fibroblasts derived from aged murine hearts, the ERK1/2 pathway alters collagen production and cell proliferation (Hung *et al.*, 2001a,b). Inhibiting ERK1/2 or JNK showed positive effects on cardiac contractility and decreased the area of fibrotic tissue and progression of myocardial fibrosis in cardiomyopathy caused by mutation in the lamin A/C gene (Wu *et al.*, 2011). Furthermore, suppression of JNK signalling reduced the increase in the mRNA levels of profibrogenic genes by aristolochic acid and reduced fibroblast proliferation in kidneys after injury (Yang *et al.*, 2010). Thus, research on the utility of targeting ERK1/2 and JNK to treat cardiac fibrosis seems worthwhile, but few experiments have been performed. Notably, simvastatin attenuated ERK1/2 activation caused by hyaluronan-mediated motility (Wang *et al.*, 2014). Additionally, several statin-treated cells show decreased ERK1/2 activity (Nemoto *et al.*, 2012; Chen *et al.*, 2013; Qi *et al.*, 2013). Inhibition of TNF-α-induced

membrane localization of Ras and RhoA by simvastatin leads to reduced phosphorylation of ERK1/2 and JNK in mouse myoblast C2C12 cells (Yamashita *et al.*, 2008). Therefore, we focused on the mechanism by which simvastatin regulates MAPK pathways.

We hypothesized that simvastatin down-regulated MAPK signalling by inducing TGFBR3 expression. Our results showed that simvastatin abolished ERK1/2 and JNK activation, which was reversed by silencing of TGFBR3 *in vitro*. Furthermore, we silenced TGFBR3 by lentivirus *in vivo* and confirmed that TGFBR3 played a critical role in the improvement of heart function, decreased collagen deposition and reduced activation of the MAPK pathway, induced by simvastatin. As a consequence, TGFBR3 was identified as the target of simvastatin in its regulation of the MAPK pathway.

The next challenge was to determine how TGFBR3 regulates ERK1/2 and JNK phosphorylation. TGFBR3 is divided into a cytoplasmic domain and an extracellular domain by the cell membrane (Gatza *et al.*, 2010). It mediates cell activities, including migration, apoptosis and invasion, through its cytoplasmic domain's interactions with specific proteins (You *et al.*, 2007). GIPC's interaction with the cytoplasmic domain of TGFBR3 via the TGFBR3 class I PDZ-binding domain stabilizes TGFBR3 levels and inhibits the TGF-β signalling that mediates cell migration and invasion (Blobe *et al.*, 2001; Lee *et al.*, 2010; Sanchez *et al.*, 2011; Townsend *et al.*, 2012). In the present study, we confirmed the interaction between TGFBR3 and GIPC. Knock-down of GIPC reversed the down-regulation of the ERK1/2 and JNK pathways by TGFBR3 over-expression. Thus, TGFBR3 affects the ERK1/2 and JNK pathways, after interaction with GIPC. Although knock-down of GIPC blocked the effects of TGFBR3 on MAPK signalling, the present study does not explain how GIPC regulates ERK1/2 and JNK pathway activation. Hu *et al.* (2003) demonstrated that GIPC directly interacts with β_1-adrenoceptors to regulate ERK1/2 activation mediated by these receptors, which may resemble the regulation of the ERK1/2 pathway by GIPC. Most notably, although we identified simvastatin as an anti-fibrotic agent in the heart by its targeting of TGFBR3, no upstream regulator of simvastatin-induced TGFBR3 expression has been identified. Our recent study showed that miR-21, a critical regulator of cardiac fibrosis development, directly down-regulated TGFBR3 and formed a positive feedback loop with TGFBR3 in cardiac fibrosis progression (Liang *et al.*, 2012). Therefore, it is worthwhile to examine whether simvastatin affects miR-21-TGFBR3 signalling in our model.

In summary, this study provides good experimental evidence that statins prevent cardiac fibrosis and that the TGFBR3/GIPC interaction is involved in statin-induced inhibition of the activation of ERK1/2 and JNK signalling. These results aid our understanding of the mechanisms by which statins protect heart function, and they reveal modulation of TGFBR3 expression in cardiac fibroblasts as a potential approach for the prevention or treatment of cardiac fibrosis.

Acknowledgements

This study was supported by the National Basic Research Program of China (973 program, 2012CB723505), the National Natural Science Foundation of China (No. 81370244; 31100826) and the Chang Jiang Scholar Candidates Programme for Provincial Universities in Heilongjiang (2013CJHB004).

Author contributions

Y. J. L. and W. F. C. designed the experiments and supervised the project. F. S., W. Q. D. and Y. Z. were primarily responsible for writing the manuscript, performing animal model, cell culture and Western blotting assays. L. L. Z. and M. G. Q. were responsible for lentivirus injection, Masson staining, electron microscope observation and echocardiographic measurement. Z. Y. L. and F. Q. were responsible for the measurement of cell viability and collagen content. D. Z. performed the statistical analysis.

Conflict of interest

The authors have no conflict of interest.

References

Alexander SPH, Benson HE, Faccenda E, Pawson AJ, Sharman JL, Spedding M *et al.* (2013a). The Concise Guide to PHARMACOLOGY 2013/14: Catalytic Receptors. Br J Pharmacol 170: 1676–1705.

Alexander SPH, Benson HE, Faccenda E, Pawson AJ, Sharman JL, Spedding M *et al.* (2013b). The Concise Guide to PHARMACOLOGY 2013/14: Enzymes. Br J Pharmacol 170: 1797–1867.

Askevold ET, Nymo S, Ueland T, Gravning J, Wergeland R, Kjekshus J *et al.* (2013). Soluble glycoprotein 130 predicts fatal outcomes in chronic heart failure: analysis from the Controlled Rosuvastatin Multinational Trial in Heart Failure (CORONA). Circ Heart Fail 6: 91–98.

Backlund T, Palojoki E, Saraste A, Eriksson A, Finckenberg P, Kyto V *et al.* (2004). Sustained cardiomyocyte apoptosis and left ventricular remodelling after myocardial infarction in experimental diabetes. Diabetologia 47: 325–330.

Blobe GC, Liu X, Fang SJ, How T, Lodish HF (2001). A novel mechanism for regulating transforming growth factor beta (TGF-beta) signaling. Functional modulation of type III TGF-beta receptor expression through interaction with the PDZ domain protein, GIPC. J Biol Chem 276: 39608–39617.

Chen J, Bi H, Hou J, Zhang X, Zhang C, Yue L *et al.* (2013). Atorvastatin overcomes gefitinib resistance in KRAS mutant human non-small cell lung carcinoma cells. Cell Death Dis 4: e814.

Chu W, Li X, Li C, Wan L, Shi H, Song X *et al.* (2011). TGFBR3, a potential negative regulator of TGF-beta signaling, protects cardiac fibroblasts from hypoxia-induced apoptosis. J Cell Physiol 226: 2586–2594.

Cleland JG, McMurray JJ, Kjekshus J, Cornel JH, Dunselman P, Fonseca C *et al.* (2009). Plasma concentration of amino-terminal pro-brain natriuretic peptide in chronic heart failure: prediction of cardiovascular events and interaction with the effects of

rosuvastatin: a report from CORONA (Controlled Rosuvastatin Multinational Trial in Heart Failure). J Am Coll Cardiol 54: 1850–1859.

Desai P, Jay A, Bock C, Dyson G, Okwuosa T, Simon MS (2013). Evaluation of the effect of genetic variation on the relationship between statins, cardiovascular disease and cancer. Int J Mol Epidemiol Genet 4: 183–192.

Esparza-Lopez J, Montiel JL, Vilchis-Landeros MM, Okadome T, Miyazono K, Lopez-Casillas F (2001). Ligand binding and functional properties of betaglycan, a co-receptor of the transforming growth factor-beta superfamily. Specialized binding regions for transforming growth factor-beta and inhibin A. J Biol Chem 276: 14588–14596.

Ezquerro IJ, Lasarte JJ, Dotor J, Castilla-Cortazar I, Bustos M, Penuelas I *et al.* (2003). A synthetic peptide from transforming growth factor beta type III receptor inhibits liver fibrogenesis in rats with carbon tetrachloride liver injury. Cytokine 22: 12–20.

Gatza CE, Oh SY, Blobe GC (2010). Roles for the type III TGF-beta receptor in human cancer. Cell Signal 22: 1163–1174.

He H, Liu X, Lv L, Liang H, Leng B, Zhao D *et al.* (2014). Calcineurin suppresses AMPK-dependent cytoprotective autophagy in cardiomyocytes under oxidative stress. Cell Death Dis 5: e997.

Hermida N, Lopez B, Gonzalez A, Dotor J, Lasarte JJ, Sarobe P *et al.* (2009). A synthetic peptide from transforming growth factor-beta1 type III receptor prevents myocardial fibrosis in spontaneously hypertensive rats. Cardiovasc Res 81: 601–609.

Hermida N, Markl A, Hamelet J, Van Assche T, Vanderper A, Herijgers P *et al.* (2013). HMGCoA reductase inhibition reverses myocardial fibrosis and diastolic dysfunction through AMP-activated protein kinase activation in a mouse model of metabolic syndrome. Cardiovasc Res 99: 44–54.

Hu LA, Chen W, Martin NP, Whalen EJ, Premont RT, Lefkowitz RJ (2003). GIPC interacts with the beta1-adrenergic receptor and regulates beta1-adrenergic receptor-mediated ERK activation. J Biol Chem 278: 26295–26301.

Hung KY, Chen CT, Huang JW, Lee PH, Tsai TJ, Hsieh BS (2001a). Dipyridamole inhibits TGF-beta-induced collagen gene expression in human peritoneal mesothelial cells. Kidney Int 60: 1249–1257.

Hung KY, Chen CT, Yen CJ, Lee PH, Tsai TJ, Hsieh BS (2001b). Dipyridamole inhibits PDGF-stimulated human peritoneal mesothelial cell proliferation. Kidney Int 60: 872–881.

Jang YH, Shin HS, Sun Choi H, Ryu ES, Jin Kim M, Ki Min S *et al.* (2013). Effects of dexamethasone on the TGF-beta1-induced epithelial-to-mesenchymal transition in human peritoneal mesothelial cells. Lab Invest 93: 194–206.

Kilkenny C, Browne W, Cuthill IC, Emerson M, Altman DG (2010). Animal research: Reporting in vivo experiments: the ARRIVE guidelines. Br J Pharmacol 160: 1577–1579.

Kong P, Christia P, Frangogiannis NG (2014). The pathogenesis of cardiac fibrosis. Cell Mol Life Sci 71: 549–574.

Kong SS, Liu JJ, Yu XJ, Lu Y, Zang WJ (2012). Protection against ischemia-induced oxidative stress conferred by vagal stimulation in the rat heart: involvement of the AMPK-PKC pathway. Int J Mol Sci 13: 14311–14325.

Krzeminski TF, Nozynski JK, Grzyb J, Porc M (2008). Wide-spread myocardial remodeling after acute myocardial infarction in rat. Features for heart failure progression. Vascul Pharmacol 48: 100–108.

Lagares D, Garcia-Fernandez RA, Jimenez CL, Magan-Marchal N, Busnadiego O, Lamas S *et al.* (2010). Endothelin 1 contributes to the effect of transforming growth factor beta1 on wound repair and skin fibrosis. Arthritis Rheum 62: 878–889.

Lee JD, Hempel N, Lee NY, Blobe GC (2010). The type III TGF-beta receptor suppresses breast cancer progression through GIPC-mediated inhibition of TGF-beta signaling. Carcinogenesis 31: 175–183.

Letamendia A, Lastres P, Botella LM, Raab U, Langa C, Velasco B *et al.* (1998). Role of endoglin in cellular responses to transforming growth factor-beta. A comparative study with betaglycan. J Biol Chem 273: 33011–33019.

Li C, Qu X, Xu W, Qu N, Mei L, Liu Y *et al.* (2013). Arsenic trioxide induces cardiac fibroblast apoptosis in vitro and in vivo by up-regulating TGF-beta1 expression. Toxicol Lett 219: 223–230.

Liang H, Zhang C, Ban T, Liu Y, Mei L, Piao X *et al.* (2012). A novel reciprocal loop between microRNA-21 and TGFbetaRIII is involved in cardiac fibrosis. Int J Biochem Cell Biol 44: 2152–2160.

McGrath J, Drummond G, McLachlan E, Kilkenny C, Wainwright C (2010). Guidelines for reporting experiments involving animals: the ARRIVE guidelines. Br J Pharmacol 160: 1573–1576.

McMurray JJ, Kjekshus J, Gullestad L, Dunselman P, Hjalmarson A, Wedel H *et al.* (2009). Effects of statin therapy according to plasma high-sensitivity C-reactive protein concentration in the Controlled Rosuvastatin Multinational Trial in Heart Failure (CORONA): a retrospective analysis. Circulation 120: 2188–2196.

Nemoto S, Taguchi K, Matsumoto T, Kamata K, Kobayashi T (2012). Pravastatin normalizes ET-1-induced contraction in the aorta of type 2 diabetic OLETF rats by suppressing the KSR1/ERK complex. Am J Physiol Heart Circ Physiol 303: H893–H902.

Olyaei A, Greer E, Delos Santos R, Rueda J (2011). The efficacy and safety of the 3-hydroxy-3-methylglutaryl-CoA reductase inhibitors in chronic kidney disease, dialysis, and transplant patients. Clin J Am Soc Nephrol 6: 664–678.

Pan Z, Sun X, Shan H, Wang N, Wang J, Ren J *et al.* (2012). MicroRNA-101 inhibited postinfarct cardiac fibrosis and improved left ventricular compliance via the FBJ osteosarcoma oncogene/transforming growth factor-beta1 pathway. Circulation 126: 840–850.

Patel R, Nagueh SF, Tsybouleva N, Abdellatif M, Lutucuta S, Kopelen HA *et al.* (2001). Simvastatin induces regression of cardiac hypertrophy and fibrosis and improves cardiac function in a transgenic rabbit model of human hypertrophic cardiomyopathy. Circulation 104: 317–324.

Pawson AJ, Sharman JL, Benson HE, Faccenda E, Alexander SP, Buneman OP *et al.*; NC-IUPHAR. (2014). The IUPHAR/BPS Guide to PHARMACOLOGY: an expert-driven knowledge base of drug targets and their ligands. Nucl Acids Res 42 (Database Issue): D1098–D1106.

Ponticos M, Holmes AM, Shi-wen X, Leoni P, Khan K, Rajkumar VS *et al.* (2009). Pivotal role of connective tissue growth factor in lung fibrosis: MAPK-dependent transcriptional activation of type I collagen. Arthritis Rheum 60: 2142–2155.

Qi XF, Zheng L, Lee KJ, Kim DH, Kim CS, Cai DQ *et al.* (2013). HMG-CoA reductase inhibitors induce apoptosis of lymphoma cells by promoting ROS generation and regulating Akt, Erk and p38 signals via suppression of mevalonate pathway. Cell Death Dis 4: e518.

Sanchez CA, Rodriguez E, Varela E, Zapata E, Paez A, Masso FA *et al.* (2008). Statin-induced inhibition of MCF-7 breast cancer cell proliferation is related to cell cycle arrest and apoptotic and necrotic cell death mediated by an enhanced oxidative stress. Cancer Invest 26: 698–707.

Sanchez NS, Hill CR, Love JD, Soslow JH, Craig E, Austin AF *et al*. (2011). The cytoplasmic domain of TGFbetaR3 through its interaction with the scaffolding protein, GIPC, directs epicardial cell behavior. Dev Biol 358: 331–343.

Shiroshita-Takeshita A, Brundel BJ, Burstein B, Leung TK, Mitamura H, Ogawa S *et al*. (2007). Effects of simvastatin on the development of the atrial fibrillation substrate in dogs with congestive heart failure. Cardiovasc Res 74: 75–84.

Shyu KG, Wang BW, Chen WJ, Kuan P, Hung CR (2010). Mechanism of the inhibitory effect of atorvastatin on endoglin expression induced by transforming growth factor-beta1 in cultured cardiac fibroblasts. Eur J Heart Fail 12: 219–226.

Sun YB, Qu X, Li X, Nikolic-Paterson DJ, Li J (2013). Endothelial dysfunction exacerbates renal interstitial fibrosis through enhancing fibroblast Smad3 linker phosphorylation in the mouse obstructed kidney. PLoS ONE 8: e84063.

Takeda N, Kondo M, Ito S, Ito Y, Shimokata K, Kume H (2006). Role of RhoA inactivation in reduced cell proliferation of human airway smooth muscle by simvastatin. Am J Respir Cell Mol Biol 35: 722–729.

Townsend TA, Robinson JY, How T, DeLaughter DM, Blobe GC, Barnett JV (2012). Endocardial cell epithelial-mesenchymal transformation requires Type III TGFbeta receptor interaction with GIPC. Cell Signal 24: 247–256.

Wang Z, Wu Y, Wang H, Zhang Y, Mei L, Fang X *et al*. (2014). Interplay of mevalonate and Hippo pathways regulates RHAMM transcription via YAP to modulate breast cancer cell motility. Proc Natl Acad Sci U S A 111: E89–E98.

Wu W, Muchir A, Shan J, Bonne G, Worman HJ (2011). Mitogen-activated protein kinase inhibitors improve heart function and prevent fibrosis in cardiomyopathy caused by mutation in lamin A/C gene. Circulation 123: 53–61.

Yamashita M, Otsuka F, Mukai T, Otani H, Inagaki K, Miyoshi T *et al*. (2008). Simvastatin antagonizes tumor necrosis factor-alpha inhibition of bone morphogenetic proteins-2-induced osteoblast differentiation by regulating Smad signaling and Ras/Rho-mitogen-activated protein kinase pathway. J Endocrinol 196: 601–613.

Yang L, Besschetnova TY, Brooks CR, Shah JV, Bonventre JV (2010). Epithelial cell cycle arrest in G2/M mediates kidney fibrosis after injury. Nat Med 16: 535–543, 531p following 143.

You HJ, Bruinsma MW, How T, Ostrander JH, Blobe GC (2007). The type III TGF-beta receptor signals through both Smad3 and the p38 MAP kinase pathways to contribute to inhibition of cell proliferation. Carcinogenesis 28: 2491–2500.

Supporting information

Additional Supporting Information may be found in the online version of this article at the publisher's web-site:

http://dx.doi.org/10.1111/bph.13166

Figure S1 Infection and expression of Lenti-shTR3 in mouse hearts. (A) Images of heart tissue expressing GFP-labelled Lenti-shTR3 7 days after infection. Tissues stained in green indicate successful Lenti-shTR3 expression. Control heart samples were extracted from age/weight-matched and sham-operated mice. (B) Expression of TGFBR3 in the hearts 0, 3, 7, 14 and 21 days after infection. (C) Expression of TGFBR3 in hearts that received Lenti-shTR3 or Lenti-shNC, treated with simvastatin for 7 days and subjected to LAD ligation for 1 week. TGFBR3 level was measured using Western blotting. Lenti-shTR3, lentivirus mediating sh-TGFBR3; Lenti-shNC, lentivirus mediating sh-NC; MI, myocardial infarction; ST, simvastatin. Data are shown as the means ± SEM. *$P < 0.05$ versus control group; #$P < 0.05$ versus MI group. †$P < 0.05$ versus MI+ST+Lenti-shNC. $n = 7$.